Chiral Textures inside 2D Achiral Domains

5 **AUTHORS**, INCLUDING:

Juan Giner-Casares
CIC biomaGUNE
46 PUBLICATIONS **281** CITATIONS

SEE PROFILE

Luis Camacho
University of Cordoba (Spain)
149 PUBLICATIONS **1,553** CITATIONS

SEE PROFILE

Chiral Textures inside 2D Achiral Domains

Eugenio Jiménez-Millan,[†] Juan J. Giner-Casares,*,[†,‡] María T. Martín-Romero,[†] Gerald Brezesinski,[‡] and Luis Camacho*,[†]

[†]Department of Physical Chemistry, University of Córdoba, Campus de Rabanales, E-14014 Córdoba, Spain
[‡]Department of Interfaces, Max Planck Institute of Colloids and Interfaces, Science Park Golm, 14476 Potsdam, Germany

Ⓢ Supporting Information

ABSTRACT: Chiral interfaces are of capital importance for biorecognition processes and nanotechnology. In this work, a mixed Langmuir monolayer was built using a surface-active dye and a phospholipid. The monolayer displayed optical activity. The driving force for the formation of the supramolecular chirality is the self-assembly of the polar headgroups of the dye. The existence of supramolecular chirality inside nonchirally-shaped domains is shown.

Chiral interfaces are of high relevance in processes of biological recognition, e.g., chiral recognition at the lipidic domains known as "lipid rafts".[1] Chirality is a current parameter of interest in nanotechnology.[2] As an interfacial platform, the Langmuir technique provides exclusive features for constructing and studying supramolecular architectures.[3]

The chirality of a particular amphiphilic molecule might be transferred to a larger scale, influencing the features of the supramolecular assemblies. The understanding of the mechanism followed by a chiral molecule that leads to a specific aggregate shape is fundamental for the bottom-up approach.[4] Previous reports have demonstrated the formation of chiral supramolecular assemblies at the air—water interface. The supramolecular assemblies display the optical activity either as guided ordering in the molecular organization[5] or as helically shaped micrometric structures.[6] Ernst has reported on the induction and remarkable further amplification of chirality in supported monolayers.[7]

In the present work, nonchiral circle-shaped domains were observed. Intriguingly, the domains display inner textures with chiral properties. In other words, the chiral supramolecular structures are enclosed within nonchiral 2D microstructures. The chirality of the inner textures is demonstrated by microscopy and circular dichroism.

The mixed Langmuir monolayer formed by the anionic phospholipid dimyristoyl phosphatidic acid (DMPA) and a cationic amphiphilic derivative of the hemicyanine dye (HSP) in an equimolar ratio is described (Figure 1).

The molecular organization at the micrometer level of the mixed monolayer was studied in situ by Brewster angle microscopy (BAM). BAM has been widely used to study chiral structures related to the organization of the hydrocarbon chains of monolayers.[4] In a standard experiment, different BAM textures are observed as a result of modifications of the refractive index arising from differences in thickness, density, and/or molecular orientation in different regions of the film. Herein, the use of BAM is innovative. The headgroup of the HSP surfactant absorbs
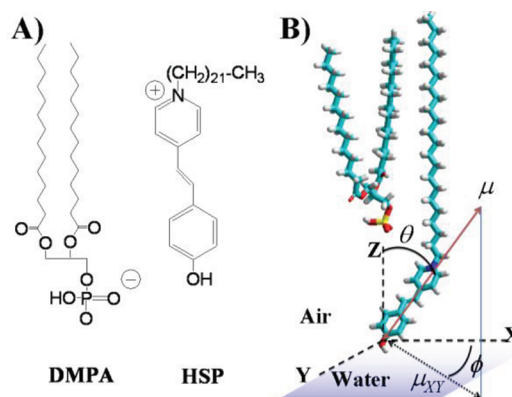

Figure 1. (A) Molecular structures of DMPA and HSP. (B) Schematic definition of the transition dipole moment, μ. The polar and azimuthal angles are denoted as θ and ϕ, respectively. The air—water interface coincides with the XY plane.

visible light at the wavelength of the BAM laser (532 nm), and this absorption is the main cause of the strong increase in the film refractivity. The BAM pictures highlight the arrangement of the polar groups of HSP as bright regions, as well as the chirality at 532 nm.

The HSP:DMPA mixed monolayer was built at the air—water interface by the cospreading method: the HSP and DMPA were dissolved in a single solution prior to the spreading of the monolayer. The occurrence of inner textures within the domains is exclusive of an equimolar ratio between the dye and the lipid. Figure 2 (top left) shows the surface pressure—area $(\pi-A)$ isotherm of the mixed monolayer. At a surface pressure of $\pi = 40$ mN/m, the surface area is $A \approx 0.6$ nm^2 per HSP molecule. This value of the area corresponds to three untilted alkyl chains: two alkyl chains per DMPA molecule plus one alkyl chain per HSP molecule (Figure 1B). Simultaneously to the isotherm recording, the morphology of the mixed monolayer at the air—water interface is observed by BAM. A gas phase and small domains are present at low surface pressures [see section S1 in the Supporting Information (SI)]. The isotherm shows an overshoot in the surface pressure at ca. 1.2 nm^2 per molecule of HSP. After the overshoot, the 2D domains are large enough to display their internal structure (Figure 2). A spiral dark region can be observed within the domains. This spiral region resembles a helix and crosses the domain vertically. Notably, the arms of the helix twist
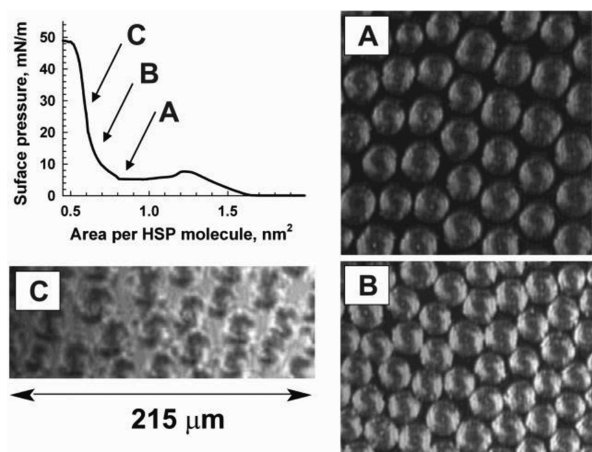
Figure 2. Surface pressure–area (π–A) isotherm of the mixed HSP:DMPA monolayer at $T = 21$ °C (top left). (A, B) BAM images with PCA = $(0°, 0°, 0°)$. (C) BAM image with PCA = $(2°, 2°, 8°)$. Image size: 215 μm width.

Figure 3. (left axis) CD spectra of four, six, and 14 HSP:DMPA monolayers transferred to a quartz support (red, blue, and green lines, respectively). (right axis) Reflection spectrum of the HSP:DMPA monolayer (black dotted line) and transmission spectrum of HSP:DMPA monolayers transferred to a quartz support (black solid line). All spectra and transfers were performed at $\pi = 30$ mN/m.

in the same direction for all domains, in an "S"-like fashion. In order to increase the resolution in the texture of the domains, the polarizer, compensator, and analyzer inclination values (PCA) from the BAM instrument were modified from PCA = $(0°, 0°, 0°)$ to PCA = $(2°, 2°, 8°)$, as shown in Figure 2C.

The inner texture of the domains indicates an anisotropic chiral organization of the HSP headgroups. The chiral structures are enclosed within the circular domains. S-shaped domains have been observed exclusively, with no occurrence of inverted S-shaped domains. For the case of a 3D supramolecular structure, both left- and right-handed helixes display identical 2D projections. However, the confinement of a chiral structure in 2D, as in the present case of a monolayer, allows the sign of rotation of the spiral to be distinguished (i.e., only one of the two possible chiral isomeric structures, which is S-shaped, is observed).

The formation of the chiral supramolecular structures from the HSP:DMPA mixed Langmuir monolayer is a complex phenomenon, with three main factors contributing. First, the HSP molecule is a prochiral molecule: it might display chirality when confined in a 2D medium.[8] The occurrence of chirality depends on the relative arrangement of the hemicyanine group in the air–water interface plane, given the all-trans configuration of the alkyl chains. In addition, the HSP molecules might show a dynamic enantiomeric conformational equilibrium due to the fact that the phenyl rings are not totally planar with respect to the double-bond plane.[9] Second, the ratio of the sizes of the polar headgroups of the constituent molecules of the mixed monolayer, DMPA and HSP, appears to play a major role. A subtle change in the molecular structure, the replacement of the $-OH$ group (HSP) with a $-N(CH_3)_2$ group (SP), negates the appearance of any inner chirality.[10] Control experiments were performed for SP(x):HSP(y):DMPA(1) mixed monolayers, where $x + y = 1$. These mixed monolayers yielded large circular anisotropic domains. Remarkably, exclusively for $y > x$, domains with chiral internal texture appeared. Some examples are provided in Figure S2 in the SI. The third factor is the inherent optical activity of the DMPA lipid. The L optical isomer of DMPA has exclusively been used herein, as this optical isomer is the only commercially available one. In this regard, control experiments with a 1:1 mixed monolayer of racemic DMPG and HSP resulted
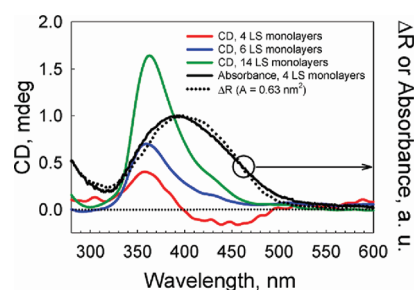
in circular domains without internal chiral textures. However, formation of some domains with chiral texture, either S-shaped or reverse-S-shaped, was observed for rac-DMPG:SP mixed monolayers (see Figure S3). The formation of chiral domains appears to depend on both the phospholipid polar group and the structure of the hemicyanine. Thus, the lipid DMPA provokes the formation of chiral domains when combined with HSP but not with SP. On the contrary, the racemic lipid DMPG (bearing a slightly bulkier polar group) forms both chiral domains with SP but not with HSP. Therefore, we conclude from the experiments that the lipid plays a critical role in the formation of the chiral structure.

In analogy to 3D crystals, previous studies have shown that either achiral molecules can yield enantiomorphous domains at the air–water interface[11] or even racemic amphiphilic α-amino acids can undergo spontaneous segregation into enantiomorphous domains on pure water or within racemic monolayers.[12]

The chiral activity of the inner textures has been studied by circular dichroism (CD) measurements. As the instrumentation does not allow the CD signal to be measured at the air–water interface, the HSP:DMPA mixed monolayer was transferred to a solid support. To rule out any change in the molecular organization during the transfer, UV–vis spectra were acquired both at the air–water interface and on the solid support. Figure 3 shows the UV–vis reflection spectrum of the HSP:DMPA monolayer at the air–water interface under a surface pressure of $\pi = 30$ mN/m. The absorption maximum appears at a wavelength of 403 nm. The HSP:DMPA monolayers were transferred onto a quartz substrate at $\pi = 30$ mN/m by the horizontal lifting or Langmuir–Schaefer (LS) method. In Figure 3, the transmission spectrum of four LS monolayers is shown. The reflection and transmission spectra do not show significant differences. Therefore, any change on the organization of the HSP headgroup during the transfer process is discarded. The lack of reorganization is important concerning the validity of the CD results (Figure S4 in the SI). Figure 3 shows the CD spectra of four, six, and 14 LS monolayers. The HSP:DMPA mixed monolayer displays optical activity.

To discard artifactual CD from birefringence effects or lineal dichroic contributions to the CD signal, BAM experiments with systematic variation of the polarization angle were performed (Figures S5 and S6 in the SI).[13] An alternative method would be Mueller matrix spectroscopy (MMS), which provides all of the information on the optical polarization properties of the molecular aggregates. However, a complete study by MMS
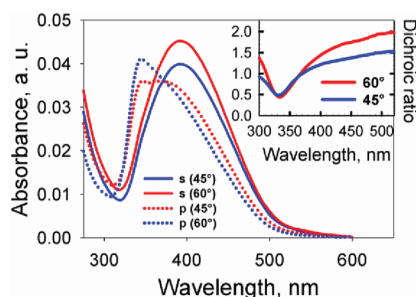
Figure 4. Polarized transmission spectra of four LS HSP:SA monolayers. The s- and p-polarized spectra are denoted as solid and dotted lines, respectively. The angles of incidence were 45° (blue) and 60° (red). Inset: Variation of the dichroic ratio (DR = Abs_s/Abs_p).

was beyond the scope of this study, although it would be of maximum interest for future research.[14] The CD spectra show the characteristic bisignate signals only for four LS monolayers (maximum at 355 nm and minimum at 430 nm) with a crossover at ∼400 nm, close to the absorption maximum. However, for six and 14 LS monolayers, the CD signals show a positive sign exclusively, with a maximum at 355 nm and a shoulder at 430 nm.

The arrangement of the HSP headgroup on the solid support is described by polarized UV−vis spectroscopy. Figure 4 shows the transmission spectra of four LS monolayers obtained at 60° and 45° incidence and s- and p-polarized light. The shapes of the spectra under s- and p-polarized light are significantly different. The differences between the s- and p-polarized spectra indicate the occurrence of anisotropy of the HSP headgroup. The s-polarized spectrum shows a broad band centered at ∼395 nm, whereas the p-polarized spectrum has a narrow band centered at 350 nm and a shoulder at ∼400 nm. The dichroic ratio, DR = Abs_s/Abs_p, is shown in Figure 4. The variation of the DR with the wavelength is due to the nonequivalent molecules in the aggregate. This phenomenon has been described previously for molecular crystals by Davidov's theory, which shows that a molecular energy level may be split into as many components as inequivalent molecules per unit cell.[15] In addition to the spectral splitting, the Davidov bands exhibit distinct polarization properties, as in the present case.

The DR at 60° incidence varies from 0.42 at $\lambda \approx 335$ nm to 2.0 at $\lambda \approx 500$ nm. In the case of 45° incidence, the DR varies from 0.49 at $\lambda \approx 335$ nm to 1.52 at $\lambda \approx 500$ nm. The polarization properties of the band are related to the coexistence of two transition dipoles with different orientations. The two transition dipoles are named the H and J components and have absorption maxima at ∼350 and ∼400 nm, respectively. The values of the polar angle θ (see Figure 1B) calculated using the DR values were found to be $\theta = 23 \pm 2°$ for $\lambda \approx 335$ nm (H component) and $\theta \approx 70 \pm 4°$ for $\lambda \approx 400$ nm (J component) (see section S8 in the SI for details). The position of the Cotton effects in the CD spectra at 355 and 430 nm are consistent with the maxima of the H (∼350 nm) and J (∼400 nm) components of the absorption spectra, indicating the existence of a supramolecular chirality in the films. The bisignate signal observed for the CD spectrum of four LS monolayers (see Figure 3) is indicative of an intense exciton coupled between the H and J components.[16] When the number of monolayers was increased, only a positive Cotton effect was observed in the CD spectra, which could be indicative of incoherent or low exciton coupling[17] due to a partial loss of order in the transferred films.
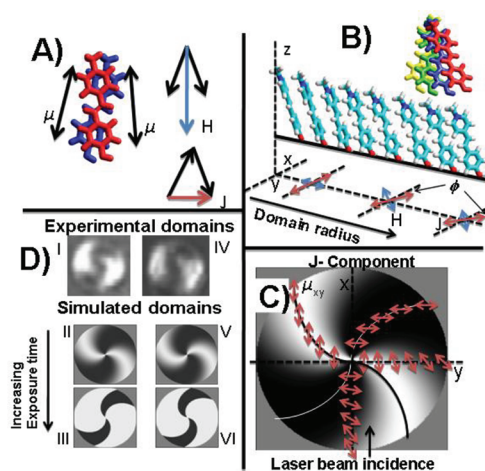

Figure 5. (A) The two optically allowed components of the addition of the transition dipoles. (B) Sketch of the hemicyanine aggregation model. The blue and red arrows represent the projections on the xy plane of the H and J components of the transition dipoles, respectively. (C) Variation of the azimuthal angle (ϕ) of the J component. (D) Zoom of the experimental and simulated domains.

In opposition to the self-aggregation tendency, two adjacent HSP molecules experience a strong repulsion between their dipole moments. To reduce this repulsion energy, partial rotation of the groups in opposite directions occurs, as sketched in Figure 5A (SP molecules are shown in different colors for clarity). The transition dipoles (μ) are not parallel. The addition of the dipoles gives rise to two optically allowed components: the H component, which is almost perpendicular to the interface (blue arrow), and the J component, which is almost parallel to the interface (red arrow). The H and J components have been described experimentally above.

Hemicyanine might form molecular linear H or J aggregates where the planes of the dye lie approximately parallel to each other.[18] However, if there is a certain distance between the planes, a slight shift between planes appears in order to reduce the repulsion energy between the dipole moments, causing rotation of the headgroups with respect to each other. In the case of a random rotation, the aggregate displays no chirality.[10] However, the molecular aggregate displays chirality when the rotation occurs in a coherent direction (Figure 5B). In the case of a linear aggregate that grows along any radius of the circular domains, the projections of the H and J components of the transition dipoles onto the xy plane will rotate along the radius (see the blue and red arrows in Figure 5B for the H and J components, respectively). This is the experimental case presented herein. The variation of the azimuthal angle ϕ corresponding to the J component is indicated in Figure 5C.

It should be noted that the absorption of the BAM laser at 532 nm from the HSP headgroups is due exclusively to the J component. Therefore, the domain textures originated from the variations of the J component, as noted in Figure 5C (μ_{xy}, red arrows). Given the x axis as the laser incidence axis (Figure 5C), high reflectivity (bright regions) is expected when μ_{xy} and the x axis are parallel, whereas low reflectivity (dark regions) is expected when μ_{xy} and the x axis are perpendicular.

A simulation of the domains observed by BAM was performed using the Fresnel equations. Details of the simulation procedure are given in section S9 in the SI. Briefly, the reflectivity for any

domain radius was assumed to change progressively as a result of the variation of ϕ. A linear variation of ϕ with distance was assumed (Figure 5B). The absolute reflectivity of the film and a relative gray-level scale were obtained. An increase in the exposure time can increase the contrast of the image (Figure 5D). The model correctly described the experimentally observed domain textures, at least qualitatively.

In summary, the formation of micrometer-sized domains at the air—water interface with achiral geometry and displaying inner chiral texture is described. This phenomenon is related to the ordered self-aggregation of the polar hemicyanine group. The rotation of the polar groups can be displayed directly within the domains. The formation of chiral supramolecular structures for the HSP:DMPA system at the air—water interface has been related to structural factors: the prochiral character of the HSP molecule and the structural relation between the components of the monolayer. The relevance of the optical activity of the L-DMPA might be significant, according to the experimental results. The rotation of the HSP headgroups to reduce the repulsion between dipole moments gives rise to the chiral textures, as confirmed by simulations. Only one of the two possible chiral isomeric structures the S-shaped one, was observed. Therefore, the chirality might be regarded as the chiral transfer from the chiral center localized in the DMPA to the chromophore. We expect these results to improve the strategy for the design of chiral supramolecular materials as well as offer new insights on chiral recognition sites at biological interfaces.

■ ASSOCIATED CONTENT

Ⓢ **Supporting Information.** Experimental details, UV—vis reflection spectra, additional BAM studies, tilt angles of the H and J components, and simulations of circular domains. This material is available free of charge via the Internet at http://pubs.acs.org.

■ AUTHOR INFORMATION

Corresponding Author
jjginer@uco.es; lcamacho@uco.es

■ ACKNOWLEDGMENT

■ REFERENCES

(1) Jacobson, K.; Mouritsen, O. G.; Anderson, R. G. W. *Nat. Cell Biol.* **2007**, *9*, 7.

(2) Guerrero-Martínez, A.; Auguié, B.; Alonso-Gómez, J. L.; Dzolic, Z.; Gómez-Graña, S.; Zinic, M.; Cid, M. M.; Liz-Marzán, L. M. *Angew. Chem., Int. Ed.* **2011**, *50*, 5499.

(3) Kuzmenko, I.; Rapaport, H.; Kjaer, K.; Als-Nielsen, J.; Weissbuch, I.; Lahav, M.; Leiserowitz, L. *Chem. Rev.* **2001**, *101*, 1659.

(4) Vollhardt, D.; Nandi, N.; Banik, S. D. *Phys. Chem. Chem. Phys.* **2011**, *13*, 4812.

(5) (a) Zhang, L.; Lu, Q.; Liu, M. H. *J. Phys. Chem. B* **2003**, *107*, 2565. (b) Yuan, J.; Liu, M. H. *J. Am. Chem. Soc.* **2003**, *125*, 5051. (c) Ribo, J. M.; Crusats, J.; Sagués, F.; Claret, J.; Rubires, R. *Science* **2001**, *292*, 2063.

(6) (a) Huang, X.; Li, C.; Jiang, S.; Wang, X.; Zhang, B.; Liu, M. *J. Am. Chem. Soc.* **2004**, *126*, 1322. (b) Vollhardt, D.; Emrich, G.; Gurberlet, T.; Fuhrhop, J.-H. *Langmuir* **1996**, *12*, 5659. (c) Nandi, N.; Vollhardt, D. *Chem. Rev.* **2003**, *103*, 4033. (d) Weissbuch, I.; Leiserowitz, L.; Lahav, M. *Curr. Opin. Colloid Interface Sci.* **2008**, *13*, 12.

(7) (a) Fasel, R.; Parschau, M.; Ernst, K.-H. *Nature* **2006**, *439*, 449. (b) Fasel, R.; Parschau, M.; Ernst, K.-H. *Angew. Chem., Int. Ed.* **2003**, *42*, 5178. (c) Parschau, M.; Romer, S.; Ernst, K.-H. *J. Am. Chem. Soc.* **2004**, *126*, 15398.

(8) Vidal, F.; Delvigne, E.; Stepanow, S.; Lin, N.; Barth, J. V.; Kern, K. *J. Am. Chem. Soc.* **2005**, *127*, 10101.

(9) Bica de Alencastro, R.; Da Motta Neto, J. D. *Int. J. Quantum Chem.* **2001**, *81*, 202.

(10) González-Delgado, A. M.; Rubia-Payá, C.; Roldán-Carmona, C.; Giner-Casares, J. J.; Pérez-Morales, M.; Martin-Romero, M. T.; Muñoz, E.; Camacho, L.; Brezesinski, G. *J. Phys. Chem. C* **2010**, *114*, 16685.

(11) Jiao, T.; Liu, M. *J. Phys. Chem. B* **2005**, *109*, 2532.

(12) (a) Rubinstein, I.; Bolbach, G.; Weygand, M. J.; Kjaer, K.; Weissbuch, I.; Lahav, M. *Helv. Chim. Acta* **2003**, *86*, 3851. (b) Weissbuch, I.; Rubinstein, I.; Weygand, M. J.; Kjaer, K.; Leiserowitz, L.; Lahav, M. *Helv. Chim. Acta* **2003**, *86*, 3867.

(13) Spitz, C.; Dähne, S.; Ouart, A.; Abraham, H. W. *J. Phys. Chem. B* **2000**, *104*, 8664.

(14) El-Hachemi, Z.; Arteaga, O.; Canillas, A.; Crusats, J.; Llorens, J.; Ribo, J. M. *Chirality* **2011**, *23*, 585.

(15) Davydov, A. S. *Theory of Molecular Excitons*; McGraw-Hill: New York, 1962.

(16) Superchi, S.; Giorgio, E.; Rosini, C. *Chirality* **2004**, *16*, 422.

(17) Guo, Z. X.; Yuan, J.; Cui, Y.; Chang, F.; Sun, W. H.; Liu, M. H. *Chem.—Eur. J.* **2005**, *11*, 4155.

(18) (a) Song, Q.; Evans, C. E.; Bohn, P. W. *J. Phys. Chem.* **1993**, *97*, 13736. (b) Lusk, A. L.; Bohn, P. W. *Langmuir* **2000**, *16*, 9131.